Accepted Manuscript

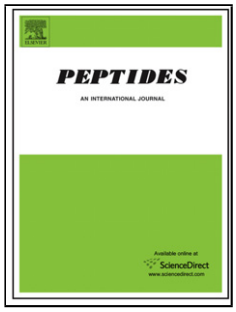

Title: Synthesis of Breast Cancer Targeting Conjugate of Temporin-SHa Analog and its Effect on Pro- and Anti-Apoptotic Protein Expression in MCF-7 Cells

Authors: Farzana Shaheen, Muhammad Nadeem-ul-Haque, Aqeel Ahmed, Shabana U. Simjee, A. Ganesan, Almas Jabeen, Zafar Ali Shah, M. Iqbal Choudhary

PII: S0196-9781(18)30128-1
DOI: https://doi.org/10.1016/j.peptides.2018.07.002
Reference: PEP 69991

To appear in: *Peptides*

Received date: 12-4-2018
Revised date: 5-7-2018
Accepted date: 5-7-2018

Please cite this article as: Shaheen F, Nadeem-ul-Haque M, Ahmed A, Simjee SU, Ganesan A, Jabeen A, Shah ZA, Choudhary MI, Synthesis of Breast Cancer Targeting Conjugate of Temporin-SHa Analog and its Effect on Pro- and Anti-Apoptotic Protein Expression in MCF-7 Cells, *Peptides* (2018), https://doi.org/10.1016/j.peptides.2018.07.002

Synthesis of Breast Cancer Targeting Conjugate of Temporin-SHa Analog and its Effect on Pro- and Anti-Apoptotic Protein Expression in MCF-7 Cells

Farzana Shaheen[†,*], Muhammad Nadeem-ul-Haque[†], Aqeel Ahmed[‡], Shabana U. Simjee[†,‡], A. Ganesan[§], Almas Jabeen[‡], Zafar Ali Shah[†], M. Iqbal Choudhary[†,‡]

[†]H. E. J. Research Institute of Chemistry, International Center for Chemical and Biological Sciences, University of Karachi, Karachi-75270, Pakistan

[‡]Dr. Panjwani Center for Molecular Medicine and Drug Research, International Center for Chemical and Biological Sciences, University of Karachi, Karachi-75270, Pakistan

[§]School of Pharmacy, University of East Anglia, Norwich Research Park, Norwich NR4 7TJ, United Kingdom

[*]**Correspondence to:** Prof. Dr. Farzana Shaheen, H.E.J. Research Institute of Chemistry, International Center for Chemical and Biological Sciences, University of Karachi, Karachi-75270, Pakistan,
Email: afnan.iccs@gmail.com
Fax: (92-21)99261713

Graphical Abstract

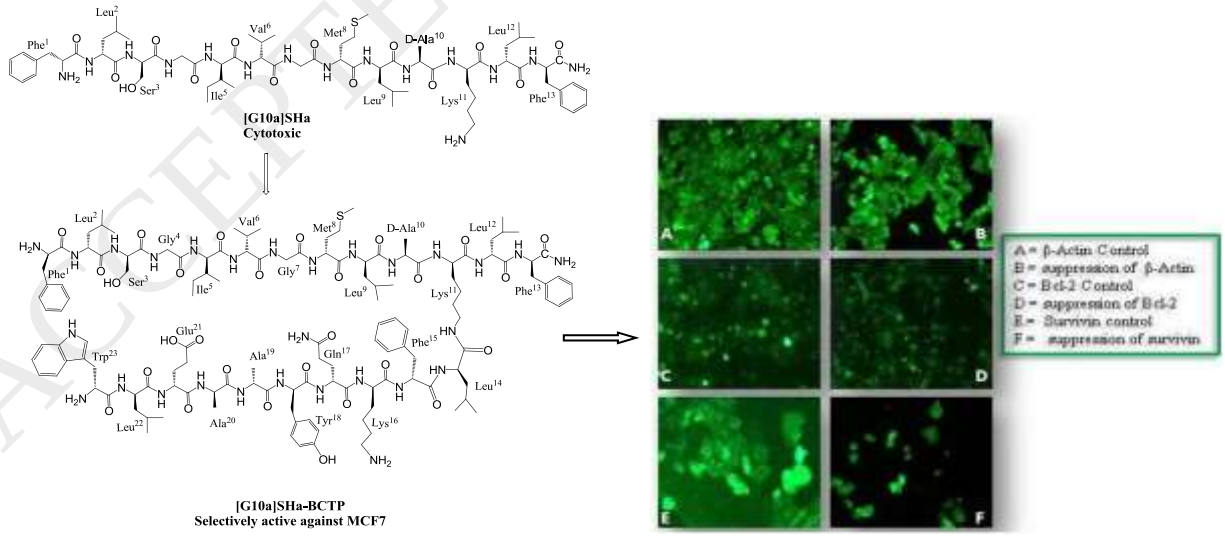

Research Highlights

- A new analog [G10a]SHa of temporin-SHa (FLSGIVGMLGKLF$_{amide}$) was found to be cytotoxic to MCF-7, HeLa, H460, 3T3 cell lines**.**
- The analog [G10a]SHa induced necrotic type of cell death in MCF7 cells.
- By conjugating the analog [G10a]SHa to the breast cancer targeting peptide, a conjugate [G10a]SHa-BCTP selective for breast cancer cells was developed which acts by inducing apoptosis.
- [G10a]SHa-BCTP up-regulated the caspase-3 and Bax expression, while down-regulated the Bcl-2 and survivin, inducing programmed type of cell death in MCF7 cells.

ABSTRACT

The frog natural product temporin-SHa (FLSGIVGMLGKLF$_{amide}$) is a potent antimicrobial peptide, as is the analog [S3K]SHa. By solid-phase synthesis, we prepared temporin-SHa and several temporin-SHa analogs with one or more D-alanine residues incorporated. The natural product and the analog [G10a]SHa were found to be cytotoxic in mammalian cell lines and induce cell death. To achieve selectivity, we conjugated the analog [G10a]SHa with a breast cancer targeting peptide (BCTP). The resulting peptide temporin [G10a]SHa-BCTP conjugate was selectively active against the MCF-7 breast cancer cell line with no cytotoxicity in NIH-3T3 fibroblasts. Unlike the natural product or [G10a]SHa, the conjugated peptide induced apoptosis, down regulating the expression of Bcl-2 and survivin and up regulating Bax and caspase-3.

Abbreviations: AMP, Antimicrobial peptides; ANOVA, Analysis of Variance; Bcl-2, B-cell lymphoma 2 (Bcl-2), Bax, BCL2 Associated X; DMSO, Dimethyl sulfoxide; TFA, Trifluoroacetic acid; FACS, Fluorescence-activated cell sorting; GAPDH, Glyceraldehyde 3-phosphate dehydrogenase; MCF-7, Michigan Cancer Foundation-7; MTT, 3-(4, 5-Dimethylthiazol-2-yl)-2,5-diphenyl tetrazolium bromide; RPMI-1640 medium, Roswell

Park Memorial Institute (RPMI) 1640 Medium; SPSS, Statistical Package for the Social Sciences.

Keywords: antimicrobial peptides, temporin-SHa analogs, breast cancer targeting peptide conjugate, apoptosis, Bcl-2, survivin, caspase-3

1. Introduction

Cancer is a condition that refers to abnormal cell growth with the potential to invade other parts of the body, and is one of the main causes of mortality worldwide. Conventional treatments include radiation or chemotherapy which often lack selectivity against cancer cells. The deleterious side effects on healthy cells and tissues cause toxicity towards vital organs and severe inflammatory responses due to necrosis [1-4]. To improve the selectivity of therapeutic agents, one strategy involves conjugation of the cytotoxic drug with targeting ligands such as antibodies or tumor targeting peptides that recognize specific receptors on particular types of cancer cells [5-12]. Recently, a decapeptide sequence WXEAAYQXFL, with varied residues at X positions, was discovered to promote specific binding to breast cancer cell lines [10-12]. One of these breast cancer targeting peptides (BCTP), with D-norleucine and D-arginine residues in positions 2 and 8 respectively, was modified (r8k and C-terminal carboxyamidation) and then conjugated with the cytotoxic anticancer drug doxorubicin. The resulting conjugate exhibited selectivity for breast cancer cell lines compared to the parent drug [11].

We were interested in applying the cancer targeting concept to antimicrobial peptides (AMPs). Although AMPs are primarily known for their antimicrobial properties, some examples and their derivatives are reported as potent antitumor agents with low toxicity such as temporin-1CEa, ascaphin-8, alyteserin-2 and magainin-2 [13-17]. These AMPs bind to the plasma membrane and cause cell death by either necrosis or apoptosis [18-21]. As a proof of concept, we started with the antimicrobial peptide temporin-SHa ($FLSGIVGMLGKLF_{amide}$). Temporin-SHa was isolated from the skin of the Sahara frog *Pelophylax saharicus* and reported as an antimicrobial agent active against bacteria, yeasts and fungi [22,23]. Temporin-SHa, the analogs temporin-[S3K]SHa and the L-alanine

substituted temporin-[A2,6,9]SHa were not found cytotoxic against mammalian cell lines such as THP-1 monocytes (IC_{50}>60 μM) and HepG2 cells (IC_{50} >600 μM) [23]. We synthesized various D-Ala substituted analogs of temporin-SHa and screened them against several cancer cell lines as well as 3T3 cells to identify analogs with anticancer activity. We then planned to conjugate the breast cancer targeting peptide (BCTP) [10-12] to the most potent analog to achieve selective targeting towards breast cancer.

2. Materials and Methods

2.1. General procedures

Resins, amino acids, and coupling reagents, were procured from Novabiochem, and Chem-impex (USA). The ^{1}H and ^{13}C NMR spectra were recorded on Bruker NMR spectrometers (Bruker, Switzerland), operating at 600 MHz and 125 MHz, respectively. HRFAB-MS was recorded on JEOL JMS HX 110 mass spectrometers (Japan). All peptides were purified by using LC-908 W recycling preparative HPLC (Japan Analytical Industry) by using a Jaigel ODS-MAT 80 (C18) column. The purity of peptides was established by Ultra-Performance Liquid Chromatography (UPLC) (Agilent 1260 Infinity Diode Array, C-4 reversed-phase analytical column, 5μm, 150 x 4.6 mm).

2.2. Peptide synthesis

Solid-phase synthesis was performed manually by using a step-wise Fmoc peptide synthesis protocol. Rink amide MBHA resin (0.51 mmol/g, Novabiochem) soaked in DCM, was first treated with 20 % 4-methylpiperidine to remove the Fmoc protecting group from Rink linker. Fmoc-protected phenylalanine (3 equiv), Oxyma pure (0.65 g, 3 equiv), and DIC (0.71 mL, 3 equiv) in 10 mL of DMF were added in the resin, and the suspension shaken overnight. Fmoc-phenylalanine loaded resin was then deprotected by 20 % 4-methylpiperidine in DMF. The resin was then treated with the next Fmoc amino acid (3 equiv.) in DMF, Oxyma pure (3 equiv.) and DIC (3 equiv.). The reaction mixture was agitated for 2 hours. Completion of reaction was checked by a ninhydrin colorimetric test. Through repeated couplings, the synthesis of all peptide sequences and [G10a]SHa-BCTP conjugate (Scheme S1) was completed with removal of the Fmoc group on the last residue. The peptides were then cleaved from the resin with 95% TFA, cocktail (94 % TFA, 1 % triisopropylsilane, 2.5 % ethanedithiol, 2.5% water) for 2 hours at room temperature. The

crude peptide was precipitated with diethyl ether and recovered from centrifugation and then lyophilized. Further purification of peptides was carried out by RP-HPLC using acetonitrile / water (60:40) in 0.1 % TFA at a flow rate of 4 mL / min.

2.3. Mass spectrometric analysis of peptides

Matrix-assisted laser desorption/ionization (MALDI) analysis was performed on an Ultraflex III TOF/TOF (Bruker Daltonics, Bremen, Germany) mass spectrometer. All peptides, dissolved in H_2O/ ACN (40:60), 0.1% TFA, were mixed with 0.5 µL of the matrix (HCCA) solution (saturated solution in 0.1% TFA/CH_3CN, 2:1), and deposited on a MALDI plate. Spectra were recorded as described earlier [24]. ESI-QTOF-MS spectra were recorded on a Q-STAR XL mass spectrometer (Applied Biosystems). Each peptide dissolved in 0.1% TFA/H_2O/ ACN 40:60 was infused directly into the mass spectrometer at a flow rate of 3 µL/min to acquire full scan and product ion mass spectra. The electrospray voltage at the spraying needle was optimized at 5500 V.

2.4. Cell lines and materials

NIH-3T3 (ATCC® CRL-1658™), NCI-H460 (ATCC® HTB-177™) and the human breast cancer cell line MCF-7 (ATCC® HTB-22™) were purchased from ATCC. MCF-7 cells were used because these cells retain many ideal characteristics particular of differentiated mammary epithelium. NCI-H460 cell line is derived from non-small cell lung carcinoma [25]. NIH-3T3 cells are mouse fibroblast cells suitable for transfection studies and can be used as a non-cancerous model for cytotoxicity studies [26]. DoHH2 cells were 1st isolated from pleural fluid of non-Hodgkin's lymphoma patient, act as representative of B-cell line (DoHH2) [27]. DoHH2 cells were kindly provided by Professor Daniel Hoessli from University of Geneva, Switzerland. HeLa cells were kindly donated by Dr. Anwar Siddiqui from Aga khan University Karachi, Pakistan. RPMI-1640 medium, FBS, and mouse anti-human-Bcl-2 primary antibody and mouse anti-human beta-actin primary antibody were purchased from Sigma-Aldrich (USA). The TRIzol reagent and Alexa Fluor® 488goat anti-mouse secondary antibody were obtained from Invitrogen (USA). Anti-human-Bax primary antibody was procured from Santa Cruz Biotechnologies (USA). DAPI, TUNEL

Assay kit, cDNA synthesis kit and SYBR green master mix, and rabbit monoclonal anti-survivin primary antibody were purchased from MP Biomedical (USA), Millipore-Merck (USA), Fermentas (USA), and Abcam (USA) respectively.

2.5. [3-(4, 5-Dimethylthiazol-2-yl)-2,5-diphenyl tetrazolium bromide] MTT assay

The cytotoxic as well as antiproliferative effect of peptides was determined using MTT [3-(4, 5-dimethylthiazol-2-yl)-2, 5-diphenyl tetrazolium bromide] colorimetric assay. Briefly MCF-7, NIH-3T3, HeLa, and NCI-H460 cells were cultured, and after confluency, cells were used to test the cytotoxicity. MTT, a tetrazolium salt, was used to check the cytotoxicity of cultured cells [28]. MTT became reduced when exposed to oxidoreductase in viable cells, and transformed into purple formazan crystals. Briefly 6000 of MCF-7 cells per well and 4000 cells of NIH-3T3, HeLa and NCI-H460 cells per well were seeded in 96-wells plate and incubated at 37ºC in 5% CO_2 for 24 h. MCF-7 cells were then treated with different doses of peptide [G10a]SHa (12.5, 25 and 50 µM) and [G10a]SHa-BCTP (25, 50 and 100 µM) and re-incubated in 5% CO_2 at 37ºC for 48 hours. The other cell lines were tested with different doses (1, 10 and 100 µM). Untreated control cells were treated with complete medium, while vehicle control cells with medium containing 0.5% DMSO. Doxorubicin, cycloheximide, and cisplatin were used as standard drugs for MCF-7, NIH-3T3 and NCI-H460, respectively. After 48 hours, media containing compounds were removed and 200 µl medium containing (0.5 mg/ml) MTT was added to each well and re-incubated for 4 h at 37 ºC in 5 % CO_2. After 4 hours, MTT containing media were removed and formazan crystals were solubilised in pure DMSO and absorbance was measured using photometer (Thermofisher, USA) at 550 nm wavelength. Experiment was performed three times and all doses were repeated in triplicate and the calculations were done using formula for percent inhibition.

$$\text{Percent Inhibition} = \frac{(\text{Absorbance of control cells} - \text{Absorbance of treated cells}) \times 100}{\text{Absorbance of control cells}}$$

2.6. Alamar blue assay

The viability of DoHH2 cells was determined by Alamar blue assay. Briefly cells were grown in RPMI media supplemented with 10% FBS and 1% penicillin/ streptomycin. Upon reaching confluence 20,000 cells per well were incubated with different concentrations (1, 10, and 100 µM) of compounds for 24 hrs. A one-tenth volume of Alamar blue was then added, and the incubation continued for 4 hrs. Absorbance was read in spectrophotometer at wavelengths of 570 nm and 600 nm [29].

2.7. DNA fragmentation assay

DNA fragmentation occurs in the last stages of apoptosis. To assess the nature of cell death by [G10a]SHa and [G10a]SHa-BCTP conjugate, TUNEL assay was performed. $2x10^6$ cells MCF-7 cells were cultured in each well of 6-well plate and kept at 37°C overnight in 5% humidified CO_2. Next day, seeded cells were treated with 0, 25, 50 and 100 µM concentrations of [G10a]SHa and G10a]SHa-BCTP conjugate for 48 hrs. Then, cells fixation was done with 1% paraformaldehyde and kept in ice 60 minutes, and then centrifuged for 5 minutes at 3000 RCF. Cell pellets were washed in PBS and 50 µL of staining solution [containing reaction buffer, terminal deoxynucleotidyl transferase (TdT) enzyme, and deoxyuridine triphosphate labeled with fluorescein (F-dUTP)] added to the pellet and placed 37 °C for 90 minutes. After incubation, cells were rinsed to remove the stain, and PI/RNase solution was incubated with cells at 1 hour. Flow cytometric analysis was performed using FACSCalibur™ instrument. Readings were taken in triplicates for each sample. Initially, singlet cells were gated by excluding doublets. Main window was set as a dot plot having FL-2 filter (for PI) on X-axis and FL-1 filter (for FITC) on Y-axis. About 95% of total cells were gated on FSC/SSC dot plot and 10000 cells were counted during each analysis. Positive control cells used in experiment were provided in the by the manufacturer (Kit number APT110, Millipore-Merck).

2.8. RNA isolation and complementary DNA synthesis

The MCF-7 cells were seeded ($1x10^6$ cells/well) in 6-well plate, and kept in 5% CO_2 at 37ºC for overnight incubation. Next day, cells were treated with medium containing 0, 25, 50, and 100 µM dose of [G10a]SHa-BCTP conjugate for 24 hrs. Total RNA was isolated using TRIzol reagent by following the manufacturer's instructions. The isolated RNA was quantified and 260/280 ratios were calculated for RNA purity using

NANOdrop®. Agarose (1.2%) gel electrophoresis was run at 70 volts for 45 minutes to determine the integrity of RNA isolated. RNA samples (1000 ng) with good integrity were used to synthesize cDNA using RevertAid®first strand kit (ThermoScientific, USA).

2.9. Gene expression analysis

Real time gene expression analysis before and after treatment with [G10a]SHa-BCTP conjugate was performed on Stratagene Mx3000p (Agilent Technologies, USA) using Maxima SYBR green (Fermentas, USA). Each reaction consisted of gene specific primers (1+1 µl), cDNA template (2 µl), nuclease free water (6 µl) and 2X SYBR master mix (10 µl). Table 1 shows the primer sequences used in this study. Bcl-2 and survivin were chosen as anti-apoptotic genes in this analysis, and Bax and caspase-3 as pro-apoptotic genes. For the normalization of data, GAPDH was used as a reference gene. All the primers were designed to have the melting temperature between 55 to 60º C. Thermal-cycling conditions were set as 95º C for 10 minutes (pre-denaturation, 1 cycle), 95º C for 15 seconds, 60º C for 30 seconds, and 72º C for 30 seconds (40 cycles). Melting curve temperatures were 95º C, 60ºC and 95º C for 14 seconds each. At the end of each extension cycle, SYBR green signals were detected, and converted automatically into ct-values. Fold change was calculated manually by using ΔΔct method:

$$\text{Fold change} = 2^{-\Delta\Delta ct}$$

Where ΔΔct = [ct of treated sample for gene of interest – ct of untreated sample for gene of interest] – [ct of treated sample for GAPDH - ct of untreated sample for GAPDH]

2.10. Immunocytochemistry

To confirm the gene expression analysis results, change in Bax, Bcl-2, survivin and beta-actin protein expression after [G10a]SHa-BCTP treatments was checked by immunocytochemistry, using a fluorescence microscope (Nikon-90i, Japan) coupled with NIS-Element Software (Nikon, Japan). Chambered slides were used to culture MCF-7 cells at a density of 4 x 10^4 cells/well. Next day, cells were incubated with 25, 50 and 100 µM doses for 48 hours. Control cells were incubated with medium only. Then, cells were washed with PBS twice and fixed with paraformaldehyde (1%) for 30 Minutes. Triton-X100 (0.5%) was used to increase the cellular membrane permeabilization for 5 minutes. Blocking was done for 10 minutes with ROTI® reagent (Carl Roth, Germany). Cells were

incubated for 90 minutes with their respective primary monoclonal antibodies (1:200 dilutions). Subsequently, cells were incubated with Alexa Fluor-488 conjugated secondary antibodies (1:200 dilutions) for 45 minutes. A set of control and treated cells were also stained with DAPI instead of antibodies. Slides were washed twice with PBS and then mounted. Images were taken using green and blue channels under 20 x lens (200x of original size).

2.11. Statistical analysis.

The data were statistically analyzed using SPSS and Microsoft Excel. Mean and standard deviation were calculated from three replicates for MTT assay, real time PCR and ImageJ readings as representatives of data. One-way ANOVA with Tukey's test was utilized to determine p-values for the significance of data.

3. Results and Discussion

3.1. Synthesis

Temporin-SHa (FLSGIVGMLGKLF$_{amide}$) and its analog [S3K]SHa are reported as potent antimicrobial peptides, while L-alanine-substituted analogs of SHa lack antibacterial and antiparasitic activities. A study regarding the antiparasitic activity of temporin-SHa revealed apoptotic cell death in *Leishmania infantum* [23]. To date, no anticancer activity of temporin-SHa or any of its analogs is reported.

Partial or entire D-amino acid substitution is reported as a useful approach to develop better therapeutic activities, to increase the resistance to proteolysis and to overcome many hurdles faced by host defense peptides [30, 31]. In the current study, the stereochemically more flexible achiral glycine residues at positions 4, 7 and/or 10 of temporin-SHa, were substituted with D-Ala residues to obtain several analogs [G4a]SHa, [G7a]SHa, [G10a]SHa, [G4,7a]SHa, [G4,7,10a]SHa, and [G7,10a]SHa (**Table 2**) through Fmoc solid-phase synthesis [31,32]. The identity was assessed by matrix-assisted laser desorption/ionization-time of flight (MALDI-TOF) mass spectrometry, HR-MALDI-TOF-MS, MALDI/MS/MS and NMR studies (Fig. S1-S16, Table S1-S9).

3.2. [G10a]SHa-BCTP showed affinity and selectivity for MCF-7 cells

Many antimicrobial peptides were reported to possess anticancer activities. However, the antimicrobial peptide temporin-SHa was reported as non-cytotoxic against the HepG2 cell line [23]. We decided to perform anticancer screening of temporin-SHa and its analogs (**Table 2**) against different cancer cell lines as well as NIH-3T3 murine fibroblast cell line (**Table 3**). Interestingly, the natural product temporin-SHa was found active against MCF-7, HeLa, and NCI-H460 cell lines with no cytotoxicity against DoHH2 cell line. The analog [G10a]SHa containing D-alanine in place of glycine at position 10 was found to be the most cytotoxic against MCF-7, HeLa and NCI-H460 cells among the peptides synthesized. Since it was cytotoxic to normal NIH-3T3 murine fibroblast cell line, we decided to improve selectivity by conjugating this peptide with the breast cancer targeting peptide (BCTP) ligand (WLEAAYQKFL) (Scheme S1), which afforded [G10a]SHa-BCTP conjugate (**Fig. 1**).

The [G10a]SHa-BCTP conjugate was fully characterized by mass spectrometry (**Table 2**) and NMR studies (Fig. S16, Table S9). The cytotoxicity of the native peptide [G10a]SHa and [G10a]SHa-BCTP conjugate was checked against MCF-7 cells at different doses (**Fig. 2**). In contrast to the native peptide [G10a]SHa, the conjugate [G10a]SHa-BCTP was active against the MCF-7 breast cancer cell line without cytotoxicity against non-cancerous cells as indicated by MTT assay results for mouse fibroblast cell line (**Table 3**). By using the reported cell-growth on-bead assay [33], we established that this peptide showed strong binding to MCF-7 cells (Fig. S17). Further studies were carried out to understand the mechanism for the increased specificity of [G10a]SHa-BCTP for MCF-7 cells.

3.3. DNA fragmentation assay

Nature of cell death induced by peptides ([G10a]SHa and [G10a]SHa-BCTP conjugate was analyzed by DNA fragmentation using standard TUNEL assay to differentiate between apoptosis and necrosis (**Fig. 3**). Cultured MCF-7 cells were treated with 0, 25, 50, and 100 µM of [G10a]SHa and [G10a]SHa-BCTP conjugate for 48 hours. The [G10a]SHa treated cells demonstrated extremely low level of DNA fragmentation, as indicated by low fluorescein labeling at all doses (**Fig. 3C, 3E and 3G**). However, intense fluorescence signals were observed for [G10a]SHa-BCTP conjugate at 25, 50 and 100 µM, thus indicating highly fragmented DNA (**Fig. 3D, 3F and 3H**) and the dot plot pattern was similar to that of the positive control cells (**Fig. 3A**).

From these observations, it can be concluded that [G10a]SHa peptide induced cell death *via* necrosis, whereas the [G10a]SHa-BCTP conjugate triggered apoptotic cell death in a dose-dependent manner. It is proposed that BCTP ligand facilitated receptor mediated delivery of [G10a]SHa-BCTP conjugate to breast cancer cells. The switching from necrosis to apoptosis may be due to the internalization of [G10a]SHa-BCTP conjugate, resulting in the delivery of peptide [G10a]SHa inside the cell to ultimately cause the induction of apoptosis.

3.4. Expression of pro- and anti-apoptotic genes following treatment with [G10a]SHa-BCTP conjugate

The results obtained from TUNEL assay indicated the apoptotic type of cell death by [G10a]SHa-BCTP conjugate and further molecular studies were performed with this peptide. Modulation in pro- and anti-apoptotic gene expression (including Bax, Bcl-2, caspase-3 and survivin) was evaluated using real time PCR after treatment with [G10a]SHa-BCTP conjugate for 24 hours. GAPDH gene expression was checked as a reference gene to normalize the data for each cDNA sample. Immunocytochemistry was performed to confirm the results at translational level.

Regulation of apoptosis is achieved by several types of proteins in a well programmed manner. Among these regulatory proteins, Bcl-2 family plays its critical role. This family includes various pro- and anti-apoptotic factors, working in a strong co-ordination in response to intra- and extracellular environmental factors. Various peptides have been studied for their impact on Bcl-2 expression in human cancer cells. Bufalin, a

peptide, has shown inhibition of ovarian tumor cells growth by down regulating Bcl-2 gene expression and Bax up-regulation [34]. In another report, a bioactive peptide, Chan Su, isolated from amphibian skin increased the expression of Bax protein and decreased Bcl-2 expression, thus resulting in apoptotic cell death [35]. In this study, the expression of Bcl-2 mRNA has been decreased significantly by [G10a]SHa-BCTP conjugate in MCF-7 cells (**Fig. 4**).This decrease in Bcl-2 expression was dose-dependent that is 0.7 and 0.6 folds at 50 and 100 µM doses, respectively. Immunocytochemistry images showed similar pattern for Bcl-2 protein expression as that was obtained at mRNA level (**Fig. 5**). Bcl-2 protein maintains the mitochondrial membrane integrity, prevent the release of cytochrome c in cytoplasm that ultimately inhibit the apoptosis to occur [36-37]. Bcl-2 protein also blocks the activity of Bak and Bax proteins (both are apoptotic) by preventing their oligomerization. Bcl-2 can inhibit both type of apoptotic pathways either apoptosome dependent or independent [38].

Few anticancer peptides have been reported for their effect on Bax protein expression [39-40]. Results obtained from gene expression analysis of Bax with [G10a]SHa-BCTP conjugate treatment showed the significant decrease in Bax gene expression that was down to 0.88, 0.75 and 0.74 folds of untreated control cells at 25, 50 and 100 µM doses, respectively (**Fig. 6**). Since we have observed significant increase in Bax gene expression after [G10a]SHa-BCTP conjugate treatment, therefore, Bax / Bcl-2 ratio was calculated for all doses (**Table 4**). These ratios become increased at 50 and 100 µM doses due to more decrease in Bcl-2 gene expression. However, fluorescence microscope images for Bax expression showed significant increase in Bax protein expression (**Fig. 7**). Immunofluorescence images of MCF-7 cells for Bax protein indicate the increase at 25 and 50 µM dose after [G10a]SHa-BCTP conjugate treatment. However, at higher doses of 100 µM dose, Bax protein expression became limited to few spots due to 48 hour treatment time. From these observations at mRNA and protein levels, it can be concluded that after [G10a]SHa-BCTP conjugate treatment, decrease in Bax gene expression might be overcome by more decrease in Bcl-2 gene expression resulting in the favorable conditions that induce apoptosis or it can be proposed that [G10a]SHa-BCTP conjugate regulates the Bax expression after transcription. Another proposed mechanism is the release of Bax protein from other protein complexes or cellular structures after

[G10a]SHa-BCTP conjugate treatment. Bax is a monomeric protein and its expression induces apoptosis in cancer cells. It resides in cytosolic part normally while in apoptosis, it becomes attached with outer mitochondrial membrane and form pores in it that ultimately releases the several factors like cytochrome c and others.

Inhibitors of apoptosis (IAPs) are also involved in regulation of apoptosis. Survivin, an IAP, plays its role in cell division cycle in tumor cells [41]. Previous studies regarding survivin expression after peptides treatment showed that down regulation of survivin induce programmed cell death [42-43]. In current study, [G10a]SHa-BCTP conjugate down regulated the survivin expression when compared with control cells. At 25 µM concentration, no change was observed (**Fig. 8**). However, at 50 and 100 µM doses, survivin expression decreased significantly down to 0.7 folds of control cells. Similarly, survivin protein expression also decreased showing a good correlation with mRNA levels. Micrographs for survivin showed the change in its arrangement with decrease in its expression after treatment with [G10a]SHa-BCTP conjugate (**Fig. 9**). In untreated control cells, survivin protein were located near the cell membrane. However, in 25 and 50 µM treated cells, expression of survivin decreased. Interestingly, at 100 µM dose, due to cell shrinkage survivin molecules aggregate together. This decrease in mRNA and protein expression clearly indicates that survivin down regulation is involved in programmed cell death at transcription as well as translation levels. Survivin exhibits its function through both extrinsic and intrinsic pathway of apoptosis (at the convergence point) and activates the caspase-3 and -7 [44].

Caspases play their critical role in apoptosis, as they activate main catalytic enzymes required for programmed cell death. Caspase-3 is the most important among all caspases. Previous studies about the effect of AMPs using solid tumor cells showed caspase-3 activation resulting in apoptotic cell death [17, 45]. Similarly, in this study, [G10a]SHa-

BCTP conjugate up-regulated the caspase-3 gene expression upto 4 to 5 folds in comparison with untreated control cells in MCF-7 cells (**Fig. 10**). This increase in caspase-3 expression is also supported by fluorescence micrographs for nuclear staining (DAPI) after treatment with [G10a]SHa-BCTP conjugate. These images indicate with increasing dose, decrease in cell number, nuclear condensation and formation of apoptotic bodies (**Fig. 11**). Being an important constituent of cytoskeleton and one of the main substrate of caspases, β-actin protein pattern and arrangement was also checked. Images for treated cells deterioration of cytoskeleton structure at higher doses that was intact in control cells image (**Fig. 12**). This destruction of β-actin protein structure, formation of apoptotic bodies and caspase-3 up-regulation validate the results obtained from TUNEL assay and confirms apoptosis induction. Caspase-3 plays its role as an executioner enzyme of caspase cascade (both extrinsic and intrinsic pathway) and further activates proteases and endonucleases. Endonucleases cut the nuclear material into short 180 bp fragments and proteases catalyze the actin structure, both helping in the formation of small apoptotic bodies.

4. Conclusions

By solid phase peptide synthesis, we prepared the frog antimicrobial peptide temporin-SHa and a series of analogs by replacing one or more glycine residues by D-alanine to improve peptide stability. Although the antimicrobial properties of temporin-SHa are well documented, we discovered that the natural peptide and analogs are inhibitors of human cancer cell lines in micromolar concentration. The highest activity was observed with [G10a]SHa and we conjugated this peptide with a breast cancer targeting peptide (BCTP) to improve selectivity. The temporin-BCTP conjugate was found to be a selective inhibitor of MCF-7 breast cancer cells. Further investigation of the mechanism revealed the conjugate induced apoptosis in MCF-7 cells through the up-regulation of caspase-3 expression and the inhibition of anti-apoptotic gene expression. Thus, conjugation to the breast cancer targeting peptide not only significantly improved the selectivity of [G10a]SHa but also switched the mechanism of cell death.

Authors' Contributions

FS designed and supervised the study. SUS and AH performed the mechanistic study of peptide conjugate. MNH synthesized and characterized all compounds reported in this study and ZAS assisted in the peptide synthesis. AG analyzed the data and interpreted the results. AJ performed cytotoxicity studies of peptides. MIC guided in the structural studies of peptides.

Funding

This work was supported by a grant 20/1656 and 5738/Sindh/NRPU/R&D/HEC/2016 from Higher Education Commission Pakistan.

Competing interest.

There are no conflicts of interest to declare.

References

1. J. Cassidy, J.L. Misset, Oxaliplatin-related side effects: characteristics and management, Semin. Oncol. 29 (2002), 11-20, https://doi.org/10.1016/S0093-7754(02)90016-3.

2. B. Kalyanaraman, J. Joseph, S. Kalivendi, S. Wang, E. Konorev, S. Kotamraju, Doxorubicin-induced apoptosis: implications in cardiotoxicity, Mol. Cell. Biochem. 234 (2002) 119-124, https://doi.org/10.1023/A:1015976430790.

3. R.P. Miller, R.K. Tadagavadi, G. Ramesh, W.B. Reeves, Mechanisms of cisplatin nephrotoxicity, Toxins 2 (11) (2010) 2490-2518, https://doi.org/10.3390/toxins2112490.

4. Y. Octavia, C.G. Tocchetti, K.L. Gabrielson, S. Janssens, H.J. Crijns, A.L. Moens, Doxorubicin-induced cardiomyopathy: from molecular mechanisms to therapeutic strategies, J. Mol. Cell. Cardiol. 52 (6) (2012) 1213-1225, https://doi:10.1016/j.yjmcc.2012.03.006.

5. B. Redko, H. Tuchinsky, T. Segal, D. Tobi, G. Luboshits, O. Ashur-Fabia, et al., Toward the development of a novel non-RGD cyclic peptide drug conjugate for treatment of human metastatic melanoma, Oncotarget 8 (1) (2017) 757-768, https://doi: 10.18632/oncotarget.12748.

6. Y. Wang, A.G. Cheetham, G. Angacian, H. Su, L. Xie, H. Cui, Peptide-drug conjugates as effective prodrug strategies for targeted delivery, Adv. Drug Deliv. Rev. 110-111 (2017) 112-126, https://doi.org/10.1016/j.addr.2016.06.015. https://doi.org/10.1016/j.addr.2016.06.015.

7. K. Bosslet, R. Straub, M. Blumrich, J. Czech, M. Gerken, B. Sperker, et al., Elucidation of the mechanism enabling tumor selective prodrug monotherapy, Cancer Res. 58 (1998) 1195-1201.

8. J. Zhang, H. Spring, M. Schwab, Neuroblastoma tumor cell-binding peptides identified through random peptide phage display, Cancer. Lett. 171 (2001) 153-164, https://doi.org/10.1016/S0304-3835(01)00575-4.

9. M. Li, W. Zhang, B. Wang, Y. Gao, Z. Song, Q.C. Zheng, Ligand-based targeted therapy: a novel strategy for hepatocellular carcinoma, Int. J. Nanomedicine 11 (2016) 5645-5669, https://doi.org/10.2147/IJN.S115727.

10. R. Soudy, A. Gill, T. Sprules, A. Lavasanifar, K. Kaur, Proteolytically stable cancer targeting peptides with high affinity for breast cancer cells, J. Med. Chem. 54 (21) (2011) 7523-7534, https://doi: 10.1021/jm200750x.

11. R Soudy, C. Chen, K. Kaur, Novel peptide–doxorubucin conjugates for targeting breast cancer cells including the multidrug resistant cells, J. Med. Chem. 56 (19) (2013) 7564–7573, https://doi: 10.1021/jm400647r.

12. R. Soudy, H. Etayash, K. Bahadorani, A. Lavasanifar, K. Kaur, Breast cancer targeting peptide binds keratin 1: A new molecular marker for targeted drug delivery to breast cancer, Mol. Pharmaceutics. 14 (2017) 593-604, https://doi:10.1021/acs.molpharmaceut.6b00652.

13. M.L. Mangoni, Temporins, anti-infective peptides with expanding properties, Cell. Mol. Life Sci. 63 (2006) 1060-1069, https://doi:10.1007/s00018-005-5536-y.

14. D.W. Hoskin, A. Ramamoorthy, Studies on anticancer activities of antimicrobial peptides, Biochim. Biophys. Acta. 1778 (2008) 357-375, https://doi.org/10.1016/j.bbamem.2007.11.008.

15. J.M. Conlon, M. Mechkarska, M.L. Lukic, P.R. Flatt, Potential therapeutic applications of multifunctional host-defense peptides from frog skin as anti-cancer, anti-viral, immunomodulatory, and anti-diabetic agents, Peptides 57 (2014) 67-77, https://doi:10.1016/j.peptides.2014.04.019.

16. Y. Qing-Zhu, W. Che, L. Lei, Z. Yang, W. He, S. De-Jing, Design of potent non-cytotoxic anticancer peptides based on the structure of antimicrobial peptide, Temporin-1CEa, Arch. Pharm. Res. 36 (2013) 1302-1310, https://doi:10.1007/s12272-013-0112-8.

17. C. Wang, Y. Zhou, S. Li, H. Li, L. Tian, H. Wang, et al., Anticancer mechanisms of temporin-1CEa, an amphipathic α-helical antimicrobial peptide, in Bcap-37 human breast cancer cells, Life. Sci. 92 (2013) 1004-1014, https://doi:10.1016/j.lfs.2013.03.016.

18. Y. Lu, T.-F. Zhang, Y. Shi, H.-W. Zhou, Q. Chen, B.-Y. Wei, et al., PFR peptide, one of the antimicrobial peptides identified from the derivatives of lactoferrin, induces necrosis in leukemia cells, Sci. Rep. 6 (2016) 20823, http://dx.doi.org/10.1038/srep20823.

19. X. Liu, Y. Li, Z. Li, X. Lan, P.H-M. Leung, J.-M, Li, et al., Mechanism of anticancer effects of antimicrobial peptides, Journal of Fiber Bioengineering and Informatics 8 (1) (2015) 25-36, https://doi:10.3993/jfbi03201503.

20. D. Gaspar, A.S. Veiga, M.A.R..B. Castanho, From antimicrobial to anticancer peptides Front. Microbiol. 4 (2013) 1-16, https://doi.org/10.3389/fmicb.2013.00294.

21. D. Ausbacher, G. Svineng, T. Hansen, M.B. Strøm, Anticancer mechanisms of action of two small amphipathic β 2, 2-amino acid derivatives derived from antimicrobial peptides, Biochim. Biophys. Acta. 1818 (11) (2012) 2917-2925, https://doi:10.1016/j.bbamem.2012.07.005.

22. F. Abbassi, C. Galanth, M. Amiche, K. Saito, C. Piesse, L. Zargarian, et al., Solution structure and model membrane interactions of temporins-SH, Antimicrobial peptides from Amphibian skin. A NMR spectroscopy and differential scanning calorimetry study, Biochemistry 47 (2008) 10513-10525, https://doi:10.1021/bi8006884.

23. Z. Raja, S. André, F. Abbassi, V. Humblot, O. Lequin, T. Bouceba, et al., Insight into the mechanism of action of temporin-SHa, a new broad-spectrum antiparasitic and antibacterial agent, PLoS ONE 12 (3) (2017) e0174024, https://doi.org/10.1371/journal.pone.0174024.

24. F. Shaheen, T.S. Rizvi, S.G. Musharraf, A. Ganesan, K. Xiao, J.B. Townsend, et al., Solid-phase total synthesis of cherimolacyclopeptide E and discovery of more potent analogues by alanine screening, J. Nat. Prod. 75 (2012) 1882-1887, https://doi:10.1021/np300266e.

25. T. Takahashi , M.M. Nau, I. Chiba, M.J. Birrer, R.K. Rosenberg, M. Vinocour, et al., p53: A frequent target for genetic abnormalities in lung cancer, Science 246 (1989) 491-494, https://doi.org/10.1126/science.2554494.

26. M. Danihelová, M. Veverka, E. Šturdík, S. Jantová, Antioxidant action and cytotoxicity on HeLa and NIH-3T3 cells of new quercetin derivatives, Interdiscip. Toxicol. 6(4) (2013) 209-216, https://doi.org/10.2478/intox-2013-0031.

27. H.C. Kluin-Nelemans, J. Limpens , J. Meerabux, G.C. Beverstock, J.H. Jansen, D. de Jong, et al., A new non-Hodgkin's B-cell line (DoHH2) with a chromosomal translocation t(14;18)(q32;q21)], Leukemia 5 (3) (1991) 221-4

28. M.B. Hansen, S.E. Nielsen, K. Berg, Re-examination and further development of a precise and rapid dye method for measuring cell growth/cell kill, J. Immunol. Methods. 119 (1989) 203-210, https://doi.org/10.1016/0022-1759(89)90397-9.

29. F. Da Roit, P.J. Engelberts, R.P. Taylor, E.C. Breij, G. Gritti, A. Rambaldi, et al., Ibrutinib interferes with the cell-mediated anti-tumor activities of therapeutic CD20 antibodies: implications for combination therapy, Haematologica 100 (1) (2015) 77-86, https://doi:10.3324/haematol.2014.107011.

30. H. Li, N. Anuwongcharoen, A.A. Malik, V. Prachayasittikul, J.E.S. Wikberg, C. Nantasenamat, Roles of D-amino acids on the bioactivity of host defense peptides, Int. J. Mol. Sci. 17 (7) (2016) 1023, https://doi.org/10.3390/ijms17071023.

31. S. Qiu, R. Zhu, Y. Zhao, X. An, F. Jia, J. Peng, et al., Antimicrobial activity and stability of protonectin with D-amino acid substitutions, J. Pept. Sci. 23 (2017) 392-402, https://doi.org/10.1002/psc.2989.

32. Z.A. Shah, S. Farooq, S.A. Ali, A. Hameed, M.I., Choudhary, F. Shaheen, New analogs of temporin LK-1 as inhibitors of multi drug resistant (MDR) bacterial pathogens, Synth. Commun. 48 (10) (2018) 1172-1182, https://doi.org/10.1080/00397911.2018.1437450.

33. N. Yao, W. Xiao, X. Wang, J. Marik, S.H. Park, K.S. Lam, Discovery of targeting ligands for breast cancer cells using the one-bead one-compound combinatorial method, J. Med. Chem. 52 (2009) 126-133, https://doi:10.1021/jm801062d.

34. K. Nasu,, M. Nishida, T. Ueda, N. Takai, S. Bing, H. Narahara, et al., Bufalin induces apoptosis and the G0/G1 cell cycle arrest of endometriotic stromal cells: a promising agent for the treatment of endometriosis, Mol. Hum. Reprod., 11(11) (2005) 817-823, https://doi.org/10.1093/molehr/gah249.

35. A. Gomes, B. Giri, A. Saha, R. Mishra, S.C. Dasgupta, A. Debnath, Bioactive molecules from amphibian skin: Their biological activities with reference to therapeutic potentials for possible drug development, Indian J. Exp. Biol. 45 (7) (2007) 579-593.

36. X. Wang, The expanding role of mitochondria in apoptosis, Genes Dev.15 (22) (2001) 2922-2933.

37. S. Cory, J.M. Adams, The BCL2 family: Regulators of the cellular life-or-death switch Nat. Rev. Cancer. 2 (2002) 647-656, https://doi:10.1038/nrc883.

38. V.S. Marsden, L. O'Connor, L.A. O'Reilly, J. Silke, D. Metcalf, P.G. Ekert, D.C.S. Huang, F. Cecconi, K. Kuida, K.J. Tomaselli, S. Roy, et al., Apoptosis initiated by Bcl-2-regulated caspase activation independently of the cytochrome c/Apaf-1/caspase-9 apoptosome, Nature 419 (2002) 634-637, https://doi:10.1038/nature01101.

39. H. Zhou, S. Forveille, A. Sauvat, V. Sica, V. Izzo, S. Durand, K. Müller, P. Liu, L. Zitvogel, O. Rekdal, et al., The oncolytic peptide LTX-315 kills cancer cells through Bax/Bak-regulated mitochondrial membrane permeabilization, Oncotarget 6 (29) (2015) 26599-26614, https://doi:10.18632/oncotarget.5613.

40. E. Paradis, H. Douillard, M. Koutroumanis, C. Goodyer, A. LeBlanc, Amyloid β peptide of Alzheimer's disease downregulates Bcl-2 and upregulates Bax expression in human neurons, J. Neurosci. 16 (23) (1996) 7533-7539, https://doi.org/10.1523/JNEUROSCI.16-23-07533.1996.

41. T.W. Owens, A.P. Gilmore, C.H. Streuli, F.M. Foster, Inhibitor of apoptosis proteins: promising targets for cancer therapy, J. Carcinog. Mutagen (2013) S14-S004 https://doi:10.4172/2157-2518.S14-004.

42. G.A. Gusarova, I.C. Wang, M.L. Major, V.V. Kalinichenko, T. Ackerson, V. Petrovic, et al., A cell-penetrating ARF peptide inhibitor of FoxM1 in mouse hepatocellular carcinoma treatment, J. Clin. Invest. 117 (1) (2007) 99-111, https://doi:10.1172/JCI27527.

43. M.B. Basse, J. Wang, F. Yu, J. Sun, Z. Li, W. Liu, Potentiation of apoptin-induced apoptosis by cecropin B-like antibacterial peptide ABPs1 in human HeLa cervical cancer cell lines is associated with membrane pore formation and caspase-3 activation, J. Microbiol. and Biotechnol. 24 (6) (2014) 756-764, http://dx.doi.org/10.4014/jmb.1209.09076.

44. I. Tamm, Y. Wang, E. Sausville, D.A. Scudiero, N. Vigna, T. Oltersdorf, et al., IAP-family protein survivin inhibits caspase activity and apoptosis induced by Fas (CD95), Bax, caspases, and anticancer drugs, Cancer Res. 58 (23) (1998) 5315-5320.

45. T.C. Huang, J.F. Lee, J.Y. Chen, Pardaxin, an antimicrobial peptide, triggers caspase-dependent and ROS-mediated apoptosis in HT-1080 cells, Mar. Drugs 9 (10) (2011) 1995-2009, https://doi:10.3390/md9101995.

Figures captions

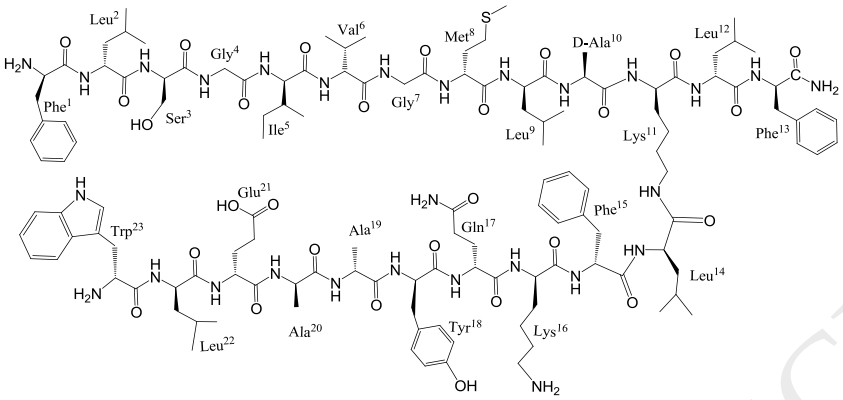

Fig. 1. Structure of [G10a]SHa-BCTP conjugate.

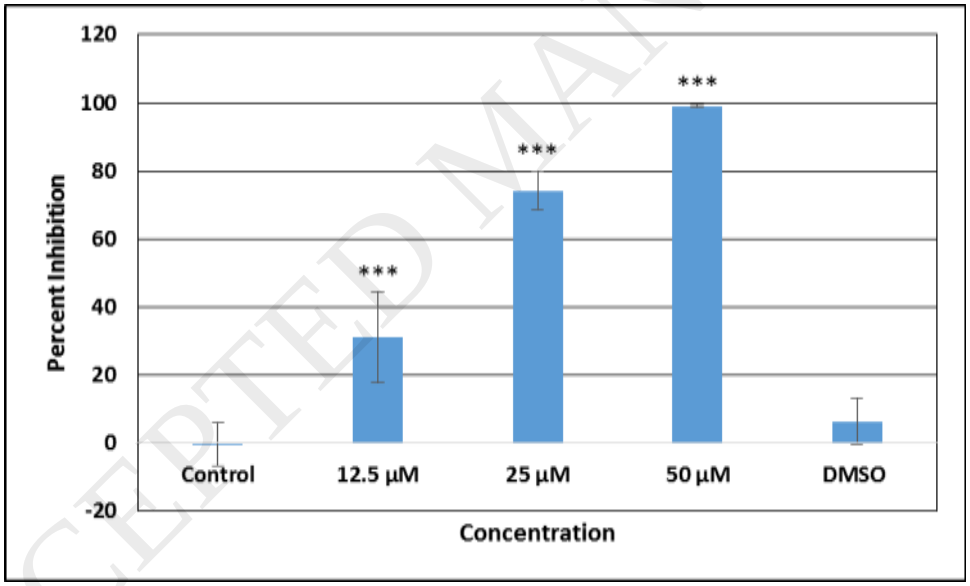

(A)

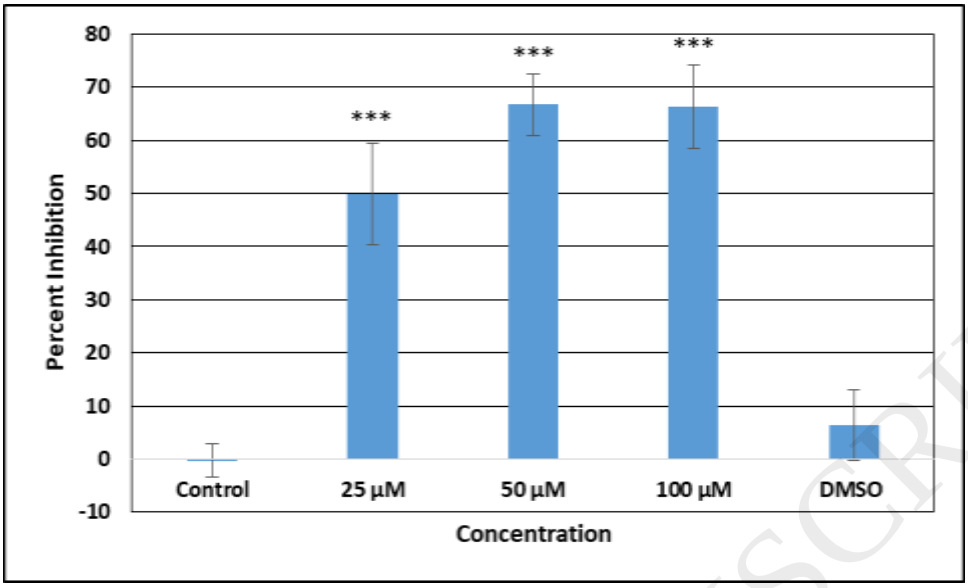

(B)

Fig. 2. Cytotoxicity of [G10a]SHa peptides against MCF-7 breast cancer cells. Fig. 2A shows cytotoxicity of [G10a]SHa, while Fig. 2B shows the cytotoxicity of the [G10a]SHa-BCTP conjugate. Data are represented as a mean of triplicates for each dose ± S.D. The concentration of DMSO used was 0.5% as it was the amount used to dissolve the highest dose of [G10a]SHa-BCTP conjugate (100 µM). One-way ANOVA reveals significant difference i.e., *$p < 0.05$, **$p < 0.01$ and ***$p < 0.001$ in comparison with control cells.

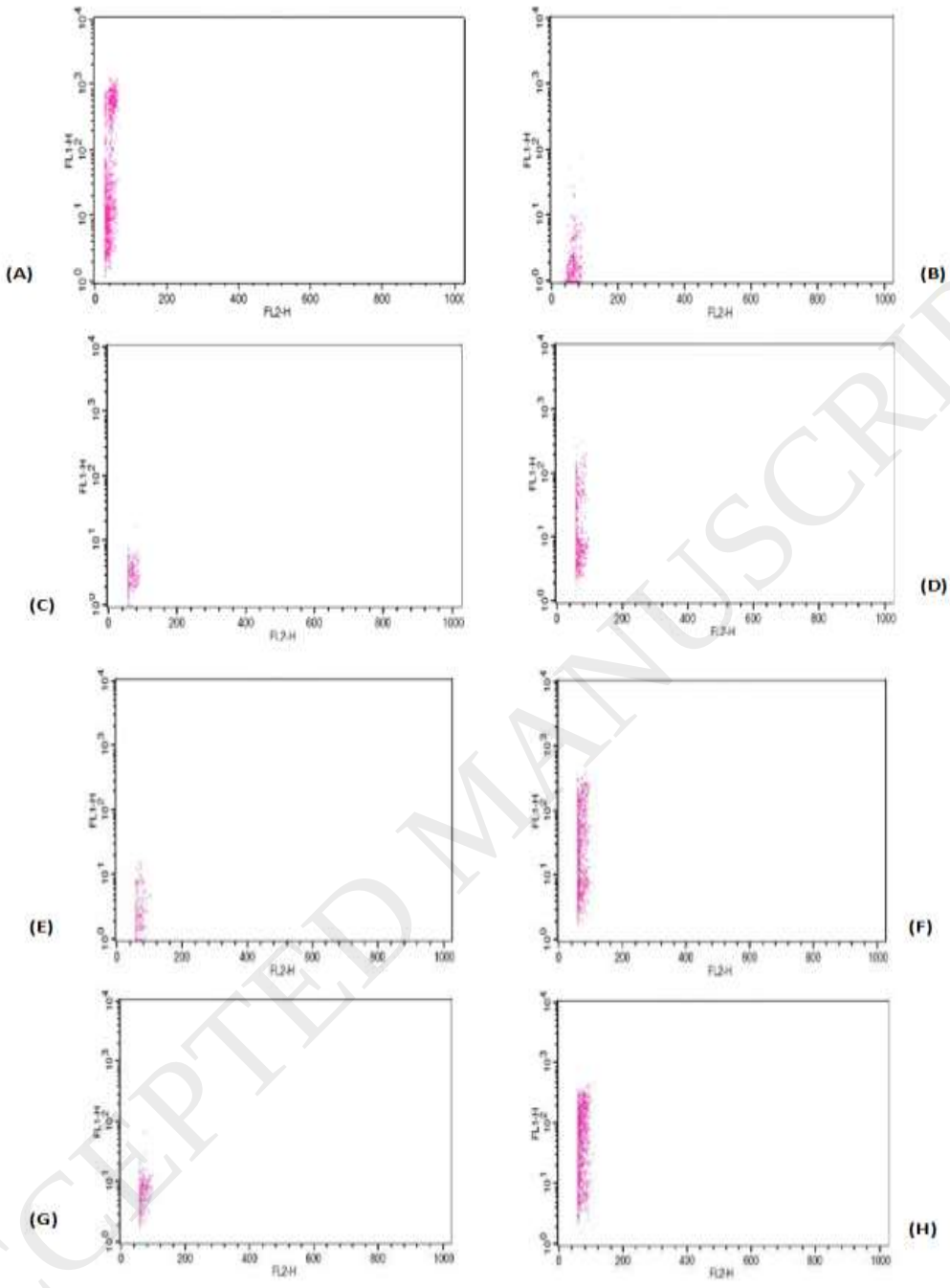

Fig. 3. TUNEL assay for [G10a]SHa and [G10a]SHa-BCTP conjugate. [G10a]SHa found to be necrotic for MCF-7 cells in Fig. 3c, 3e and 3g (25, 50 and 100 µM doses of [G10a]SHa, respectively). On the other hand, intense DNA fragmentation after [G10a]SHa-BCTP conjugate treatment showed apoptotic cell death (Fig. 3D, 3F and 3H showing 25, 50 and 100 µM doses of [G10a]SHa-BCTP conjugate , respectively). Fig. 3A represents the positive control cells. Control cells were treated with complete medium (Fig. 3B). Total 95% cells were gated and 10000 cells were counted for each case.

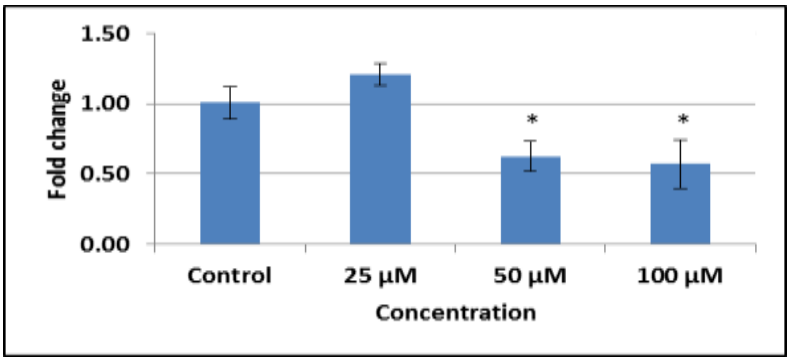

Fig. 4. Bcl-2 gene expression in [G10a]SHa-BCTP treated MCF-7 cells. RT-PCR was performed for Bcl-2 gene in triplicate for all doses and data was normalized using GAPDH. Cells incubated with complete medium only are represented by the bar labelled as Control. Data represents the mean of triplicates ± Standard deviation. One-way ANOVA was used for significant difference (i.e. * denotes p-value less 0.05, ** denotes p-value less 0.01 and *** denotes p-value less 0.001) when comparing treated samples with control cells.

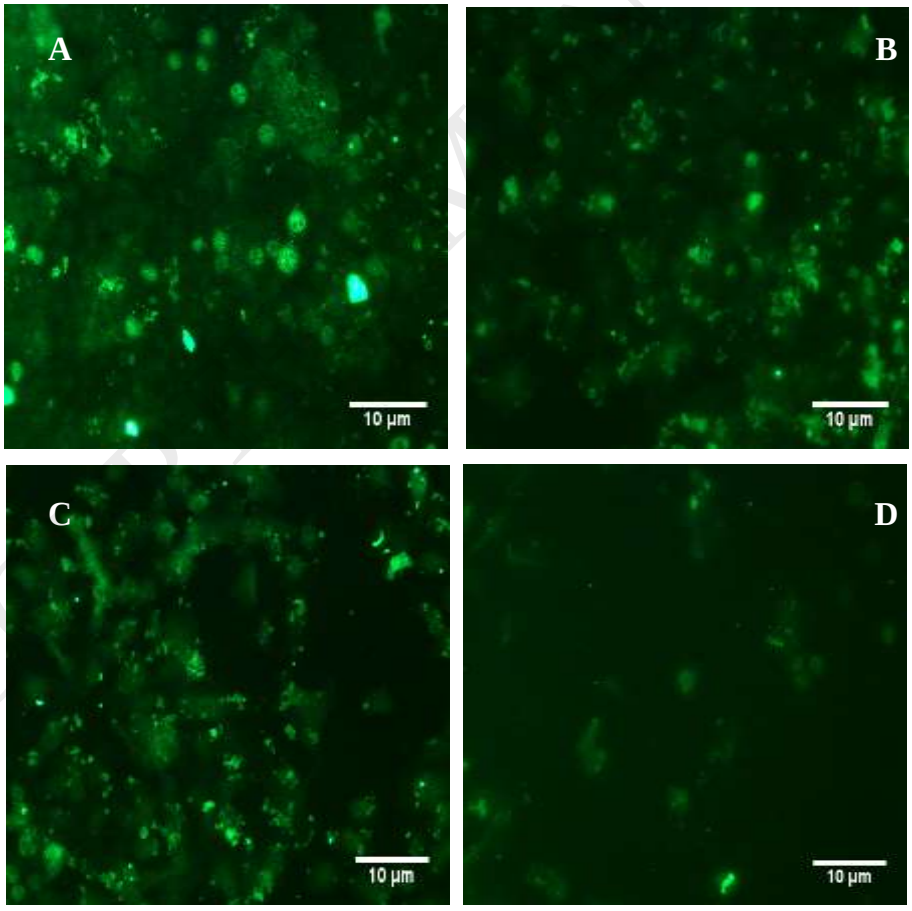

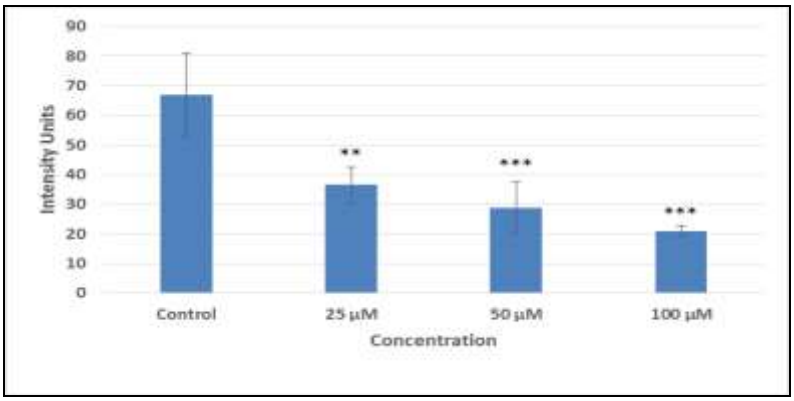

(E)

Fig. 5. Bcl-2 expression in [G10a]SHa-BCTP treated MCF-7 cells. (A) Untreated control cells; (B, C and D) Cells treated with 25, 50 and 100 µM of [G10a]SHa-BCTP conjugate. Cells were then fixed, incubated with Bcl-2 primary/secondary antibodies and images were taken using fluorescence microscope (Nikon 90i microscope). Image J software was used to quantify the intensity of fluorescence light produced by images (Fig. E).

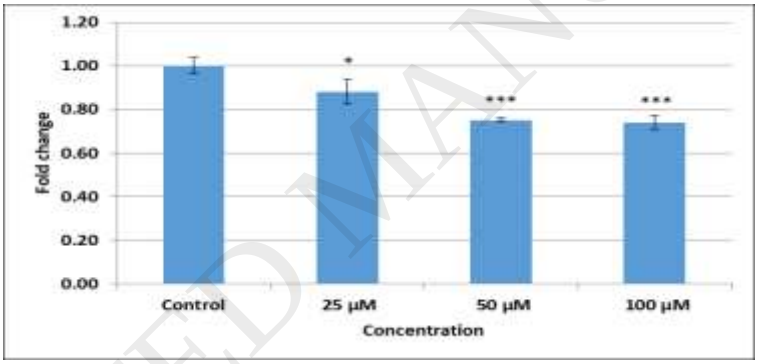

Fig. 6. Bax gene expression in [G10a]SHa-BCTP treated MCF-7 cells. RT-PCR was performed for Bax gene in triplicate for all doses and data was normalized using GAPDH. Cells incubated with complete medium only are represented by the bar labeled as Control. Data represents the mean of triplicates ± Standard deviation. One-way ANOVA was used for significant difference (i.e. * denotes p-value less 0.05, ** denotes p-value less 0.01 and *** denotes p-value less 0.001) when comparing treated samples with control cells.

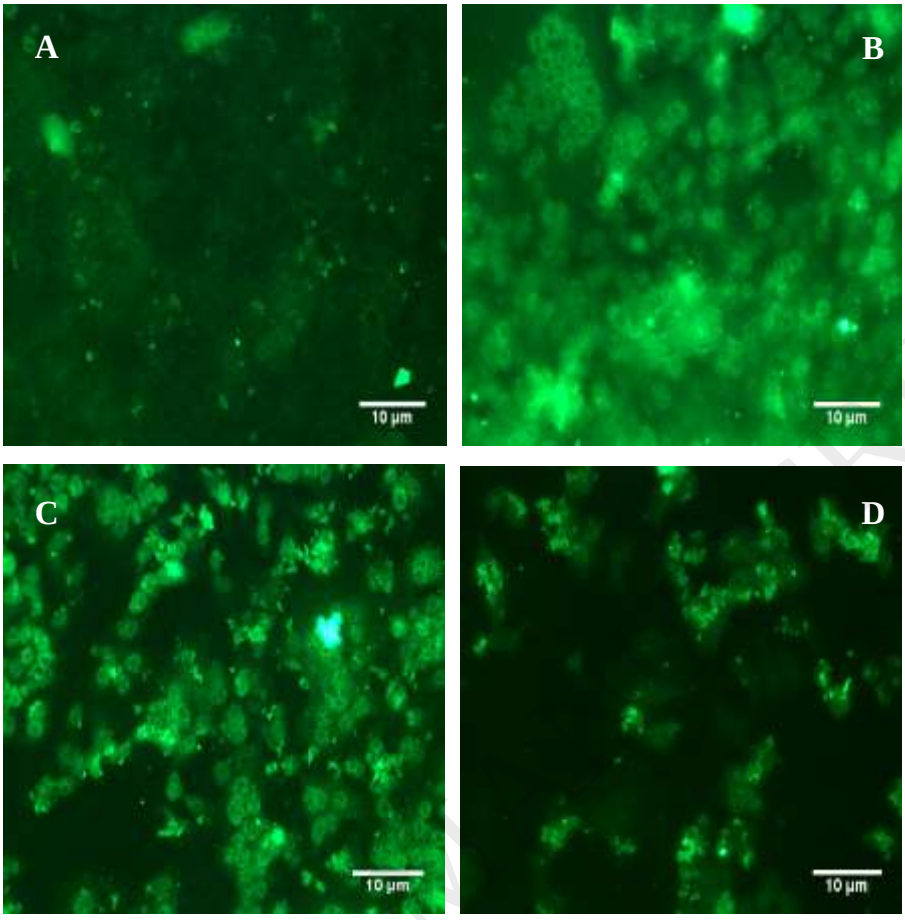

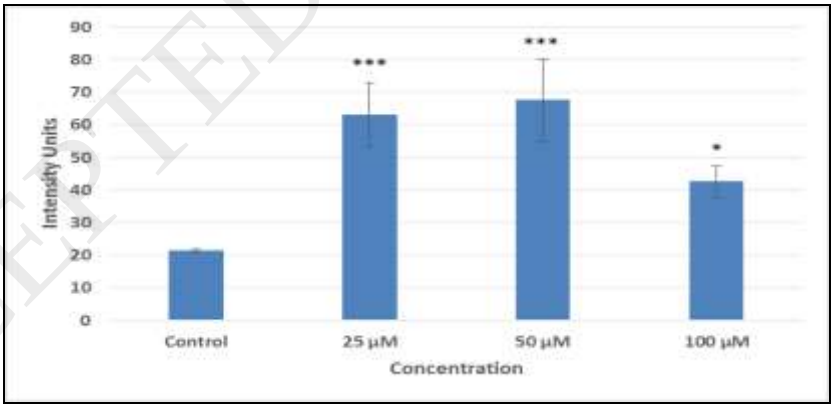

(E)

Fig. 7. Bax expression in [G10a]SHa-BCTP treated MCF-7 cells. (A) Untreated control cells; (B, C and D) Cells treated with 25, 50 and 100 µM of [G10a]SHa-BCTP conjugate. Cells were then fixed, incubated with Bax primary/secondary antibodies and images were taken using fluorescence microscope (Nikon 90i microscope). Image J software was used to quantify the intensity of fluorescence light produced by images (Fig. E).

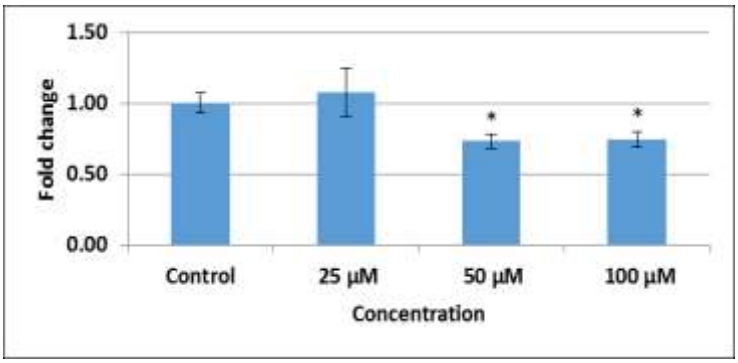

Fig. 8. Gene Expression of survivin in [G10a]SHa-BCTP treated MCF-7 cells. RT-PCR was performed for survivin gene in triplicate for all doses and data was normalized using GAPDH. Cells incubated with complete medium only are represented by the bar labelled as Control. Data represents the mean of triplicates ± Standard deviation. One-way ANOVA was used for significant difference (i.e. * denotes p-value less 0.05, ** denotes p-value less 0.01 and *** denotes p-value less 0.001) when comparing treated samples with control cells.

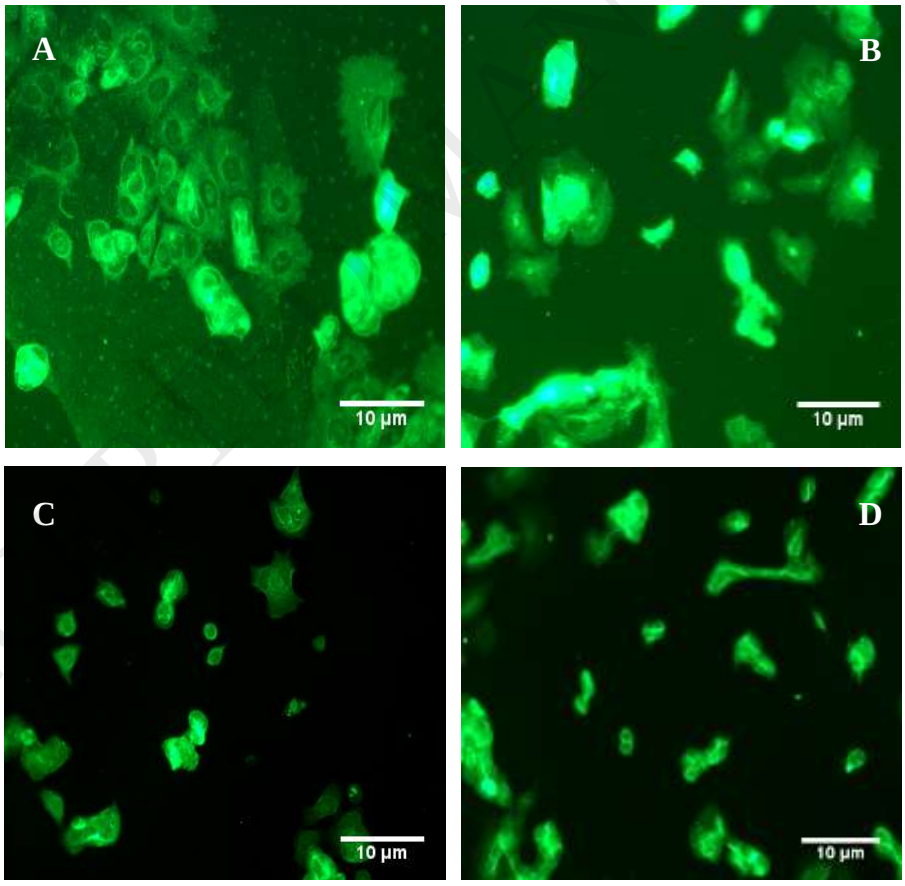

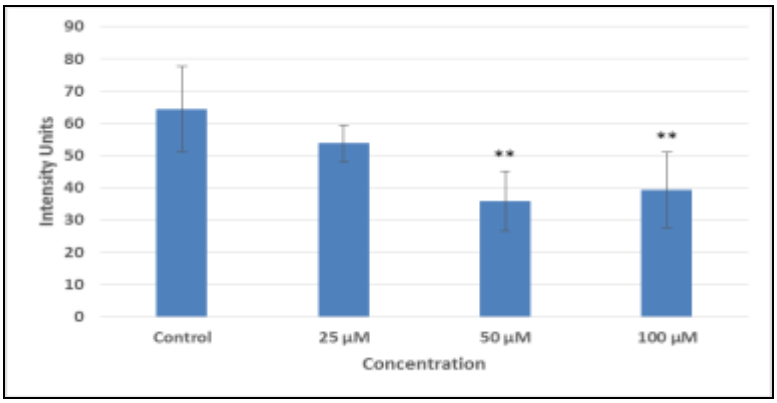

(E)

Fig. 9. Survivin expression in [G10a]SHa-BCTP treated MCF-7 cells. (A) Untreated control cells; (B, C and D) Cells treated with 25, 50 and 100 µM of [G10a]SHa-BCTP conjugate. Cells were then fixed, incubated with survivin primary/secondary antibodies and images were taken using fluorescence microscope (Nikon 90i microscope). ImageJ software was used to quantify the intensity of fluorescence light produced by images (Fig. E).

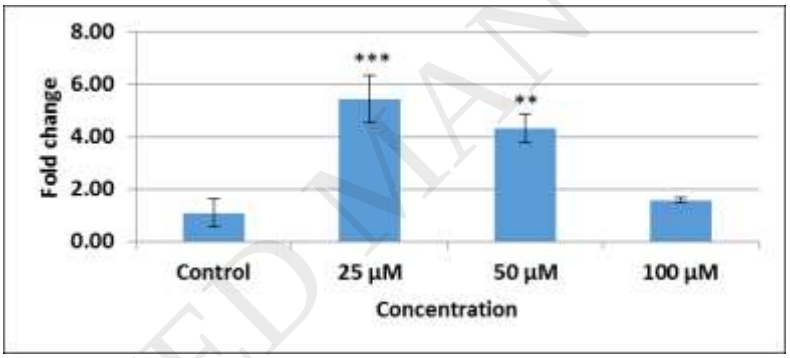

Fig. 10. Caspase-3 gene expression in [G10a]SHa-BCTP treated MCF-7 cells. RT-PCR was performed for caspase-3 gene in triplicate for all doses and data was normalized using GAPDH. Cells incubated with complete medium only are represented by the bar labeled as Control. Data represents the mean of triplicates ± Standard deviation. One-way ANOVA was used for significant difference (i.e. * denotes p-value less 0.05, ** denotes p-value less 0.01 and *** denotes p-value less 0.001) when comparing treated samples with control cells.

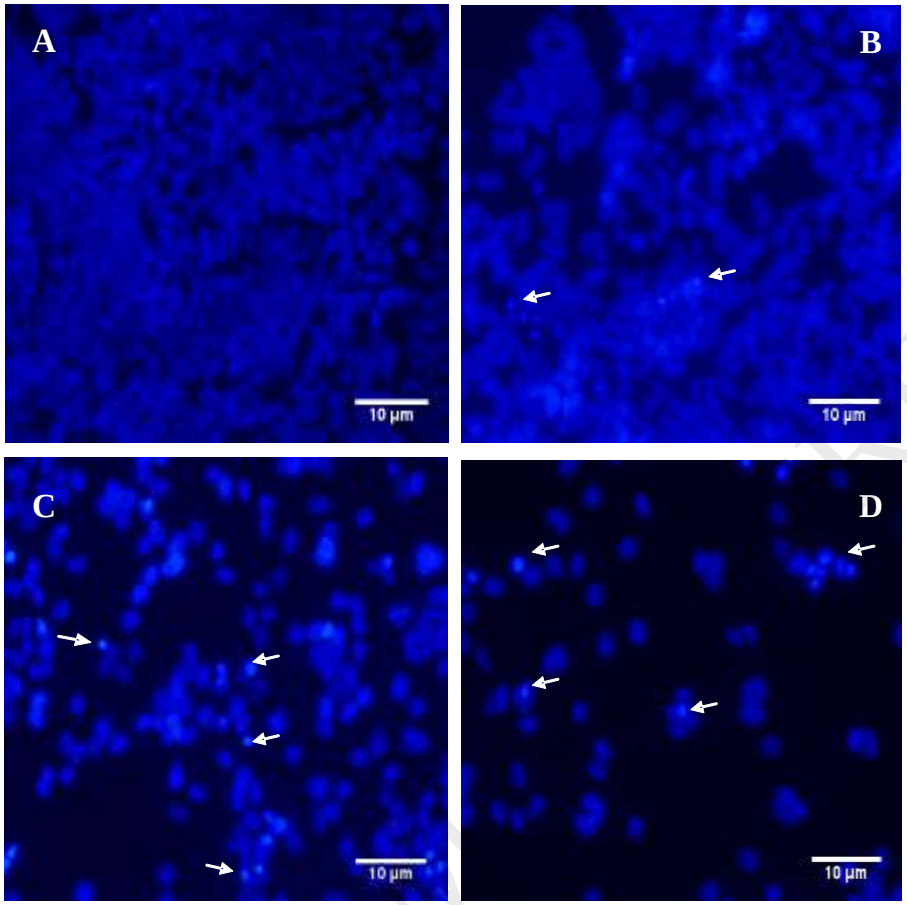

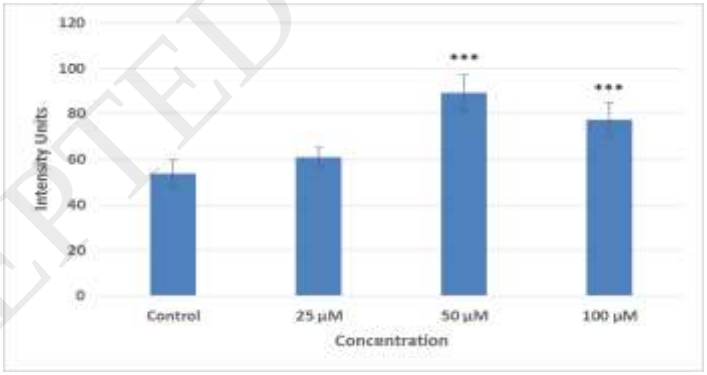

(E)

Fig. 11. Nuclear staining of [G10a]SHa-BCTP treated MCF-7 cells with DAPI. (A) Untreated control cells; (B, C and D) Cells treated with 25, 50 and 100 µM of [G10a]SHa-BCTP conjugate. Cells were then fixed, stained with DAPI and images taken using fluorescence microscope (Nikon 90i microscope). Condensation of nuclear material and formation of smaller apoptotic bodies are indicated by arrow heads. Image J software was used to quantify the intensity of fluorescence light produced by images (Fig. E).

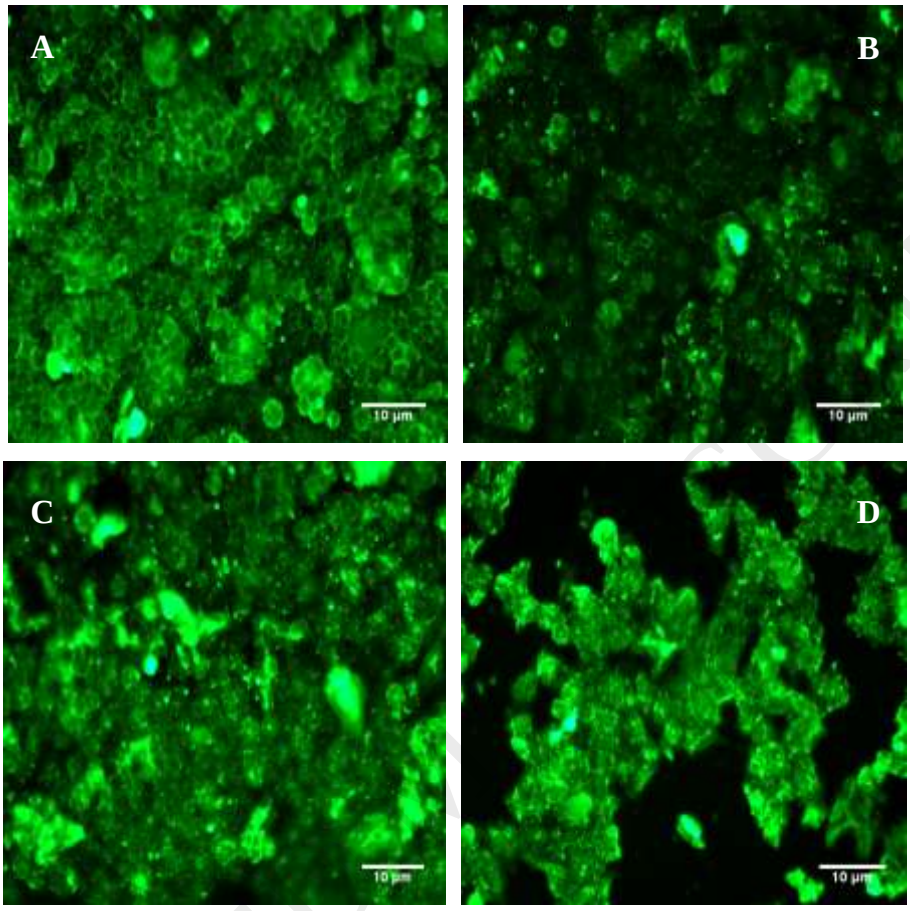

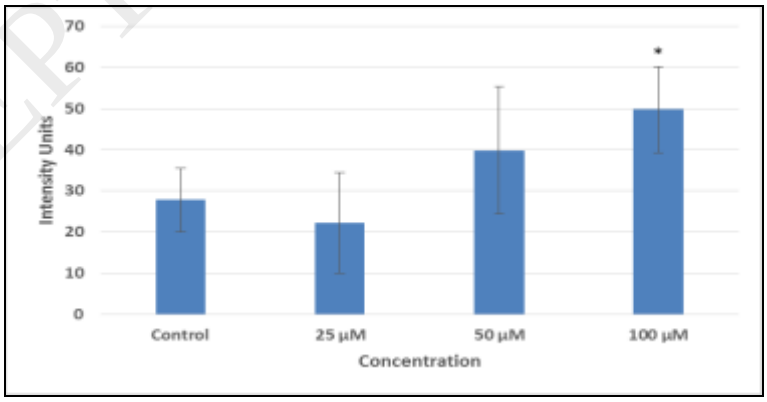

(E)

Fig. 12. β-actin expression in [G10a]SHa-BCTP treated MCF-7 cells. (A) Untreated control cells; (B, C and D) Cells treated with 25, 50 and 100 µM of [G10a]SHa-BCTP conjugate. Cells were then fixed, incubated with β-actin primary/secondary antibodies and images were taken using fluorescence

microscope (Nikon 90i microscope). Image J software was used to quantify the intensity of fluorescence light produced by images (Fig. E).

Table

Table 1

List of primers

S. No	Primer	Left	Right
1	**Bcl-2**	5´-gaggattgtggccttctttg-3´	5´-acagttccacaaaggcatcc-3´
2	**Caspase-3**	5´-atggaagcgaatcaatggac-3´	5´-atcacgcatcaattccacaa-3´
3	**Bax**	5´-agatcatgaagacaggggcc-3´	5´-gcaatcatcctctgcagctc-3´
4	**Survivin**	5´-cagagtccctggctcctctac-3´	5´-ggctcactgggcctgtcta-3´
5	**GAPDH**	5´-ccagaacatcatccctgcct-3´	5´-cctgcttcaccaccttcttg-3´

Table 2

Characterization Data of peptides

No.		Mol. Formula	Obs. mass	Calc. Mass	HRMS	Overall Yield (%)
1	Temporin-SHa	Phe[1]-Leu[2]-Ser[3]-Gly[4]-Ile[5]-Val[6]-Gly[7]-Met[8]-Leu[9]-Gly[10]-Lys[11]-Leu[12]-Phe[13]-NH_2	$[M+Na]^+$ 1402.8	1402.789	1402.789	37.0
2	[G4a]SHa	Phe[1]-Leu[2]-Ser[3]-D-Ala[4]-Ile[5]-Val[6]-Gly[7]-Met[8]-Leu[9]-Gly[10]-Lys[11]-Leu[12]-Phe[13]-NH_2	$[M+Na]^+$ 1416.8	1416.805	1416.804	68.5
3	[G7a]SHa	Phe[1]-Leu[2]-Ser[3]-Gly[4]-Ile[5]-Val[6]- D-Ala[7]-Met[8]-Leu[9]-Gly[10]-Lys[11]-Leu[12]-Phe[13]-NH_2	$[M+Na]^+$ 1416.9	1416.805	1416.808	69.6
4	[G10a]SHa	Phe[1]-Leu[2]-Ser[3]-Gly[4]-Ile[5]-Val[6]-Gly[7]-Met[8]-Leu[9]- D-Ala[10]-Lys[11]-Leu[12]-Phe[13]-NH_2	$[M+H]^+$ 1394.9	1394.823	1394.822	81.6
5	[G4,7a]SHa	Phe[1]-Leu[2]-Ser[3]- D-Ala[4]-Ile[5]-Val[6]- D-Ala[7]-Met[8]-Leu[9]-Gly[10]-Lys[11]-Leu[12]-Phe[13]-NH_2	$[M+Na]^+$ 1430.8	1430.820	1430.820	80.2
6	[G4,7,10a]SHa	Phe[1]-Leu[2]-Ser[3]- D-Ala[4]-Ile[5]-Val[6]- D-Ala[7]-Met[8]-Leu[9]- D-Ala[10]-Lys[11]-Leu[12]-Phe[13]-NH_2	$[M+Na]^+$ 1444.8	1444.836	1444.836	27.9
7	[G7,10a]SHa	Phe[1]-Leu[2]-Ser[3]-Gly[4]-Ile[5]-Val[6]- D-Ala[7]-Met[8]-Leu[9]-D-Ala[10]-Lys[11]-Leu[12]-Phe[13]-NH_2	$[M+Na]^+$ 1430.83	1430.820	1430.820	37.7
8	[G10a]SHa-BCTP conjugate	Phe[1]-Leu[2]-Ser[3]-Gly[4]-Ile[5]-Val[6]-Gly[7]-Met[8]-Leu[9]- D-Ala[10]-Lys[11]-Leu[12]-Phe[13]-NH_2 | Phe[15]-Leu[14] Trp[23]-Leu[22]-Glu[21]-Ala[20]-Ala[19]-Tyr[18]-Gln[17]-Lys[16]-	$[M+Na]^+$ 2666.5	2666.454	2666.454	22.1

Note: capital letters showing L amino acids and small letters are representatives of D configuration.

Table 3

Cytotoxicity studies of temporin-SHa analogs and [G10a]SHa-BCTP conjugate (IC_{50} in µM)

No.	NIH-3T3	MCF-7	HeLa	NCI-H460	DoHH2
Temporin-SHa	73.3 ± 0.007	14.47 ± 0.57	18.36 ± 0.92	34.5 ± 1.5	>100
[G4a]SHa	>100	17.9 ± 1.1	>100	>100	>100
[G7a]SHa	>100	22.4 ± 2.2	>100	>100	>100
[G10a]SHa	16.02 ± 3.7	16.2 ± 2.2	22.7 ± 0.86	24.3 ± 0.8	>100
[G4,7a]SHa	>100	29.5 ± 6.03	>100	37.3 ± 3.5	>100
[G4,7,10a]SHa	>100	26.33 ± 5.8	>100	>100	>100
[G7,10a]SHa	7.5 ± 0.03	21.3 ± 1.13	>100	>100	>100
[G10a]SHa-BCTP conjugate	>100	26.85 ± 1.85	>100	>100	>100
Cycloheximide	0.46 ± 0.07	-	-	-	-
Doxorubicin	-	1.6 ± 0.2	5.7 ± 0.36	-	-
Cisplatin	-	-	-	10.3 ± 0.6	-
Imatinib	-	-	-	-	42.5 ± 3.5

Table 4

Ratio of Bax/Bcl-2 in MCF-7 cells treated with [G10a]SHa-BCTP conjugate at 25, 50 and 100 µM doses

	Bax (Mean ± St. Dev)	Bcl-2 (Mean ± St. Dev)	Bax /Bcl-2
Control	1.00 ± 0.04	1.00 ± 0.11	0.99
25 µM	0.88 ± 0.06	1.20 ± 0.08	0.73
50 µM	0.75 ± 0.01	0.63 ± 0.11	1.20
100 µM	0.74 ± 0.03	0.57 ± 0.17	1.30